Concerted Hydrogen-Bond Dynamics in the Transport Mechanism of the Hydrated Proton: A First-Principles Molecular Dynamics Study

Timothy C. Berkelbach
Department of Chemistry, Columbia University, New York, New York 10027, USA

Hee-Seung Lee
Department of Chemistry and Biochemistry, University of North Carolina, Wilmington, North Carolina 28403, USA

Mark E. Tuckerman[*]
Department of Chemistry and Courant Institute of Mathematical Sciences, New York University, New York, New York 10003, USA

(Received 17 June 2009; published 30 November 2009)

First-principles molecular dynamics calculations performed in a fully converged basis set are used to reveal new details about the mechanism of the anomalous proton-transport process in water, a fundamental question dating back over 200 years. By separating actual structural diffusion from simple rattling events, wherein a proton shuttles forth and back in a hydrogen bond, it is found that the former are driven by a concerted mechanism in which hydronium begins to accept a hydrogen bond from a donor water molecule while the proton-receiving water molecule simultaneously loses one of its acceptor hydrogen bonds. The kinetics of the process are found to be in good agreement with recent experiments.

DOI: 10.1103/PhysRevLett.103.238302 PACS numbers: 82.20.Wt, 66.10.−x, 82.30.Rs

Proton transfer and the migration of both positive and negative topological charge defects in hydrogen-bonded (HB) networks are fundamental to a myriad of processes in chemistry, physics, and biology. Examples include properties of acidic and basic solutions [1], fuel-cell operation [2], and signal transduction [3]. The guiding mechanistic picture dates back over 200 years to the seminal work of C. J. T. von Grotthuss, and while first-principles [4], semiempirical [5], and reactive force-field [6] simulations have attempted to elucidate many aspects of such structural diffusion mechanisms, a complete microscopic molecular picture remains elusive.

The basic idea of von Grotthuss is that proton transport occurs not by the diffusion of free protons but rather by the migration of a topological defect in the water HB network via a sequence of proton-transfer (PT) reactions, a process known as *structural diffusion*. Despite its ingenuity, this picture is necessarily incomplete and leaves open the question of what drives this mechanism in water and what are the associated time scales. Generally, there is little question that the dynamic nature of the HB network in water must play a crucial role in determining the precise first and/or second solvation-shell rearrangements that must occur as part of the structural diffusion process [7–14]. The prevailing picture is one in which each PT step is initiated by a reduction of the coordination number of a water molecule in the first solvation shell of the hydronium atom from 4 to 3 by loss of an acceptor HB [7–9]. This reduction in coordination number creates a ‘‘symmetric’’ solvation pattern between the hydronium and one of its first solvation-shell water molecules, thereby symmetrizing the local free-energy profile [15] and leading to the interconversion of an Eigen cation or $H_9O_4^+$ complex to a Zundel cation or $H_5O_2^+$ complex. This basic picture can be refined by including more solvation shells [14,16].

While there is validity in this picture, it is unable to differentiate between actual charge-displacement events and nonproductive events in which the proton simply returns to the oxygen atom (of the hydronium ion) from which it originated, perhaps even after making a full excursion across the hydrogen bond (termed a ‘‘rattling’’ event [13] or ‘‘special-pair’’ dance [14]). What is clearly needed is a mechanistic picture that correctly describes actual charge-displacement events, and one method for approaching this problem is via first-principles molecular dynamics (FPMD), in which the finite-temperature dynamics of a system are generated with forces computed ‘‘on the fly’’ from electronic structure calculations [17]. Within this approach, both chemical-bond breaking or forming events and electronic polarization are included implicitly.

Recently, we developed an orthonormal real-space basis set approach for FPMD calculations that employs discrete variable representation (DVR) functions [18,19]. When the electronic structure is represented within a Kohn-Sham (KS) density functional theory (DFT) description, the scheme uses a direct product of DVRs to expand the KS orbitals together with a transformation to reciprocal space for evaluation of long-range interactions. This technique allows FPMD calculations with fully converged basis sets to be performed straightforwardly and efficiently. We have shown that this approach improves the description of both the structure [20] and dynamics [21] of liquid water over underconverged plane-wave calculations [22,23]. We now employ the DVR approach to investigate the mechanism of proton transport in water, which is timely as recent experiments [24] have provided relevant time scales associated with the PT process. By explicitly separating rattling from productive charge-displacement events, we find a new mechanism in which that the latter are driven by a concerted mechanism involving solvent reorganization at both the proton donor and acceptor sites. The kinetics of our new mechanism are found to be in good agreement with experiment.

We have studied a system of 31 water molecules and one hydronium (H_3O^+) in a cubic periodic box having an edge length of 9.87 Å, which provides a reasonable description of two solvation shells [20]. The electronic structure is represented within the KS DFT, with the exchange functional of Becke [25], the correlation functional of Lee, Yang, and Parr [26], and Troullier-Martins pseudopotentials [27]. The KS orbitals are expanded in a DVR basis having 75 basis functions along each coordinate direction, corresponding to a DVR grid spacing of 0.13 Å. We showed previously [20] that this basis set is sufficient to converge both the total energy and atomic forces for water within this description and system size. The initial configuration was taken from the end of a very long plane-wave based calculation [28] and then equilibrated for 40 ps in the canonical ensemble using a Nosé-Hoover chain thermostat [29] on each degree of freedom. Following this, a 70 ps microcanonical run was performed in order to analyze the dynamics of the structural diffusion process. In all simulations, hydrogens were assigned the mass of deuterium to reduce quantum effects not treated here. All calculations were carried out using the PINY_MD code [30].

In order to verify that the DVR-based approach leads to an adequate description of the hydrated proton, we show, in Fig. 1(a), the mean-square displacement of the charge defect. This plot accounts for the fact that the oxygen core (denoted O^*) of the hydronium ion changes identity with each PT reaction. From the slope of the linear region, the diffusion constant we predict is 0.80 $\text{Å}^2/\text{ps}$, which is in good agreement with the experimental value of 0.67 $\text{Å}^2/\text{ps}$ [31] and improves on previous plane-wave based calculations [28,32]. Since the value of the diffusion constant is dominated by the structural diffusion component rather than the hydrodynamic one, this level of agreement gives us confidence that the converged DVR basis set provides a good description of the structural diffusion process.

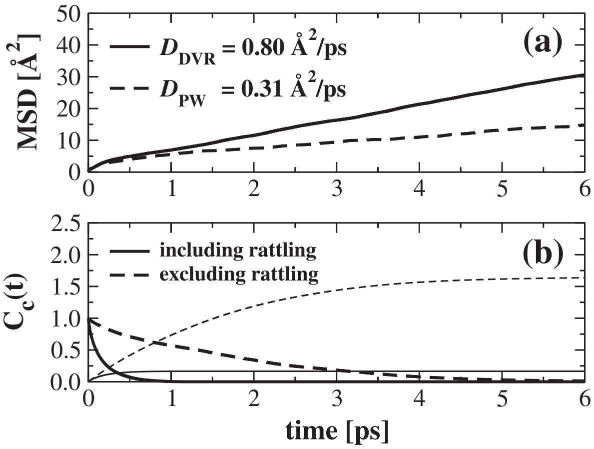

FIG. 1. Mean-square displacement (a) of the hydronium oxygen, O^*. Results are shown for the current DVR-based study (solid line) and an analogous plane-wave-based study using the protocol of Ref. [28] (dashed line), along with the calculated diffusion constants. Continuous population correlation function (b) (see text) with rattling events included (solid line) and excluded (dashed line). Thinner solid and dashed lines indicate the integrated correlation functions corresponding to the exchange lifetime τ_{exch} with and without rattling, respectively.

We next employ a recently proposed population correlation function analysis [13] to extract relevant time scales of the proton-transport process. A continuous correlation function is defined as $C_c(t) = \langle h(0)H(t)\rangle/\langle h\rangle$, where $h(t) = 1$ if a given oxygen is O^* at time t and 0 if it is not O^*, and $H(t) = 1$ if a given oxygen *remains* O^* for a time t and 0 if it does not. Integration of $C_c(t)$ gives an average O^* lifetime, τ_{exch}. A direct evaluation of this correlation function and associated lifetime results in the solid curves in Fig. 1(b), with $\tau_{\text{exch}} = 165$ fs. This short lifetime is in good agreement with the experimentally obtained Eigen-Zundel interconversion lifetime, <100 fs [24]. Note, however, that this is not a measure of the actual O^* lifetime, as the charge defect does not actually migrate on this time scale. This observation brings us to the important matter of proton rattling.

By excluding proton rattling (i.e., ignoring O^* identity changes which are undone when the *next* PT event is a return to O^*), we recompute the (now pseudo-) continuous correlation function, which integrates to a much longer lifetime, $\tau_{\text{exch}} = 1.7$ ps [dashed curves, Fig. 1(b)]. NMR experiments have estimated the H^+ hopping time to be 1.3 ps [9,33], which accords well with our calculated deuterated lifetime when isotopic factors are applied. Additionally, experimental measurements of solvent reorganization time in water have found time scales and HB lifetimes on the order of 1–2 ps [34–36]. This agreement with our calculated τ_{exch} verifies the strong dependence of proton transport on solvation-shell structure and dynamics and provides an example of the important distinction between significant charge defect migration and simple proton rattling events.

To facilitate the analysis, previous studies [10,13] employed a special oxygen denoted O', chosen as follows. We first define an asymmetric stretch reaction coordinate, $\delta = r_{\text{OH}} - r_{\text{O}^*\text{H}}$, which is calculated over all three nearest-neighbor oxygens of O^*. The oxygen for which δ is minimum is O' and is identified as the oxygen most likely to receive a transferring proton (note that $\delta = 0$ corresponds to an equally shared proton). Prior analysis of the hydrogen-bonding (H-bonding) patterns of O' showed a great similarity to those of O^*. These findings led to the "presolvation" concept described above, where the receiving oxygen must lose a HB in order to assume the

H-bonding pattern of the species into which it will be transformed via PT. It is important to note, however, that the analysis of O′ H-bonding patterns depends on the inclusion or exclusion of rattling events. Specifically, during rattling events, the transient O′ is essentially O*. As such, the O′ recorded H-bonding patterns taken over the entire simulation will very strongly reflect those of O*. Such results do not definitively conclude that HB breaking is a precursor to PT events. Despite this rattling event contamination, further analysis to follow will show that the "presolvation" concept retains substantial validity but requires modification to fully explain the dynamics of true structural diffusion.

Here, we refine the analysis of the structural diffusion process by shifting our focus from O′ to $O^*_{\rm next}$, where $O^*_{\rm next}$ is the next oxygen to become O*. Because we are concerned with the H-bonding patterns that drive PT events (i.e., O* identity changes), it makes sense to use our knowledge of the completed trajectory and observe $O^*_{\rm next}$. Nonetheless, the rattling problem persists for $O^*_{\rm next}$ for the same reasons described above for O′. During rattling events, the transient $O^*_{\rm next}$ will strongly resemble O* leading to O*-like H-bonding statistics. We can exclude rattling events by the same procedure used in generating Fig. 1(b).

To analyze the local liquid structure of O*, we employ the radial distribution function (RDF) $g_{AB}(r)$ of atom B relative to atom A and the corresponding integrated coordination number (ICN) $n_{AB}(r) = 4\pi\rho_B \int_0^r dRR^2 g_{AB}(R)$; ρ_B is the number density of atom type B. Figure 2 shows $g_{O^*_{\rm next}H}(r)$ and $n_{O^*_{\rm next}H}(r)$ averaged over 20 fs intervals well before a PT event (500–480 fs) and at the approach of a PT event (180–160 fs, 60–40 fs, and 20–0 fs), all with rattling events excluded. Data are also shown for the two other nearest neighbors of O* for comparison. Each time interval represents an average over *all* nonrattling PT events. The time progression shows the steady decrease in the $O^*_{\rm next}$H coordination number as the PT event is approached, indicating a loss of approximately one acceptor HB and hence a change in the water coordination number from 4 to 3. In addition, the HB peak shifts to the left, indicating the formation of the Zundel cation structure. By contrast, the $O_{\rm other}$ RDFs show negligible change over the time intervals.

Having clarified the role of coordination number reduction in the first solvation shell of O*, we now augment the analysis to provide a more complete picture of the structural diffusion process. Following a PT event, the previous O* must eventually assume a fourfold coordination state. In many cases, however, O* is actually found to accept a hydrogen bond *before* it transfers one of its excess protons. These results are captured in the RDF $g_{O^*H}(r)$ and ICN $n_{O^*H}(r)$ shown in Fig. 3 for same time intervals as in Fig. 2 (also averaged over *all* nonrattling PT events). These show an increase in the O*H coordination number as the PT event is approached. When compared to its counterparts averaged over the entire simulation (not shown) and at times long before the transfer [panel (a)], the O*H RDF at the time of transfer is noticeably greater in the range $r \approx$ 1.5–2.5 Å, suggesting the acceptance of a HB by O*.

This combination of HB patterns (i.e., transfers taking place into threefold coordinated water molecules and away from fourfold coordinated hydronium molecules) provides evidence for a concerted mechanism, driven by HB breaking and forming at different sites. From Figs. 2 and 3, these HB rearrangements occur within approximately 50 fs of each other. An example of a concerted PT event taken directly from the simulation is shown in Fig. 4. Panel (a) shows the hydronium and a fourfold coordinated first solvation-shell water. Panels (b) and (c), which occur in rapid succession, show the breakage of an acceptor HB in the first solvation shell and the acceptance of an HB by the hydronium. Finally, in (d), the proton hops, leaving behind

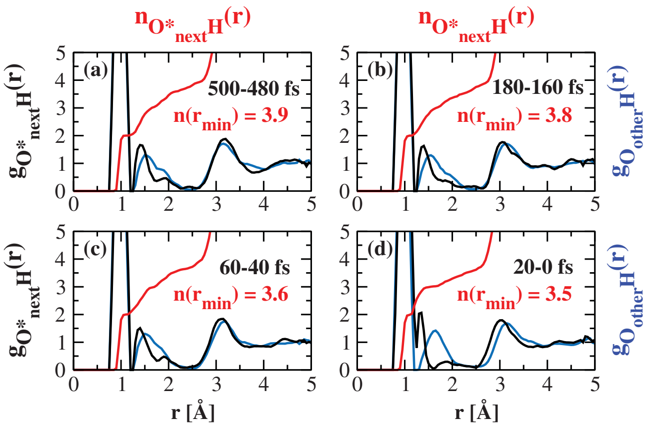

FIG. 2 (color). RDFs and ICNs of $O^*_{\rm next}$ (black and red, respectively) and RDFs for the two other nearest neighbors of O* (blue) averaged over 20 fs intervals for long times before a PT event (500–480 fs) and for intervals prior to and approaching a PT event (180–160 fs, 60–40 fs, and 20–0 fs). PT occurs in panel (d).

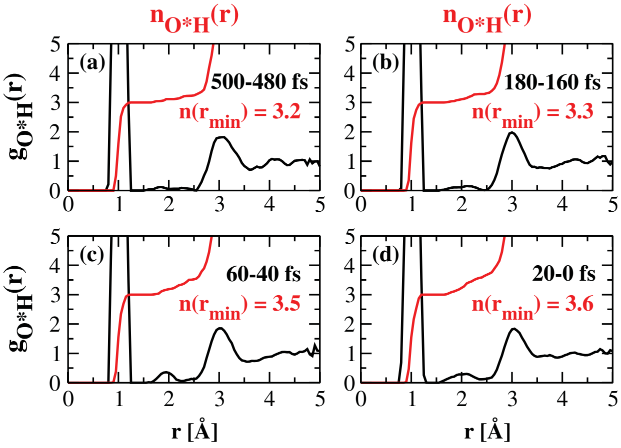

FIG. 3 (color). RDFs and ICNs of O* (black and red, respectively) averaged over 20 fs intervals for long times before a PT event (480–500 fs) and for intervals approaching a PT event (160–180 fs, 40–60 fs, and 0–20 fs). PT occurs in panel (d).

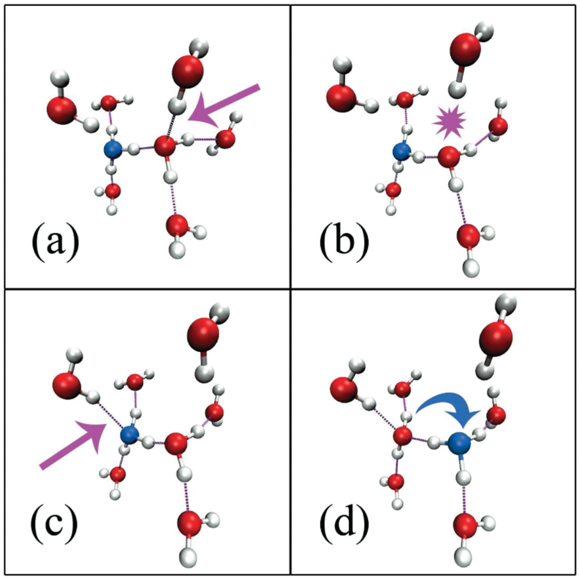

FIG. 4 (color). Snapshots of an example proton-transfer event from the actual simulation. O* is blue, oxygen atoms are red, hydrogen atoms are white, and HBs are purple. See text for mechanistic details.

a fourfold coordinated water molecule and forming a threefold coordinated hydronium at O^*_{next}. Our simulation protocol yields an O* diffusion constant and τ_{exch} in excellent agreement with experiment and shows that coordination reduction is a precursor to nearly all true structural diffusion events. More importantly, it also provides evidence of a new driving force, the donation of a HB to O*.

A concerted PT mechanism of the type shown in Fig. 4 bears some similarity to a mechanism recently proposed by Laage and Hynes for the exchange of HBs in pure water [37,38]. In their "jump reorientation" mechanism, these authors suggest that the reorienting water molecule breaks one of its donor HBs with an overcoordinated first solvation-shell water and forms a new donor HB with an undercoordinated second solvation-shell water molecule. The time scale for the actual jump is approximately 250 fs, slightly longer than the time scale for the PT events observed here. The time scale for actual charge-displacement events is also similar to the decay of the orientational correlation functions from the extended jump model. The similarity in time scales indicates the central role of water dynamics in both processes. The parallel between the two models is compelling: Fluctuations at two locations in the HB network lead to unfavorable coordination states of both O* and O^*_{next} followed by a rapid PT, which restores the more favorable local coordination patterns and prevents back transfer via rattling. This new molecular picture should provide a sound basis for understanding and controlling proton transport in related physical, chemical, and biological systems.

The authors acknowledge support from NSF Grant No. CHE-0704036 (M. E. T.), the Barry M. Goldwater Program (T. C. B.), and UNCW startup funds (H. S. L.).

*mt33@nyu.edu

[1] M. Eigen, Angew. Chem. **3**, 1 (1964).
[2] K. D. Kreuer *et al.*, Chem. Rev. **104**, 4637 (2004).
[3] C. A. Wraight, Biochim. Biophys. Acta **1757**, 886 (2006).
[4] D. Marx, Chem. Phys. Chem. **7**, 1848 (2006).
[5] G. A. Voth, Acc. Chem. Res. **39**, 143 (2006).
[6] B. Roux, Acc. Chem. Res. **35**, 366 (2002).
[7] M. E. Tuckerman *et al.*, J. Chem. Phys. **103**, 150 (1995).
[8] M. E. Tuckerman *et al.*, J. Phys. Chem. **99**, 5749 (1995).
[9] N. Agmon, Chem. Phys. Lett. **244**, 456 (1995).
[10] D. Marx *et al.*, Nature (London) **397**, 601 (1999).
[11] T. J. F. Day, U. W. Schmitt, and G. A. Voth, J. Am. Chem. Soc. **122**, 12 027 (2000).
[12] H. Lapid *et al.*, J. Chem. Phys. **122**, 014506 (2005).
[13] A. Chandra, M. E. Tuckerman, and D. Marx, Phys. Rev. Lett. **99**, 145901 (2007).
[14] O. Markovitch *et al.*, J. Phys. Chem. B **112**, 9456 (2008).
[15] P. M. Kiefer and J. T. Hynes, J. Phys. Chem. A **108**, 11 793 (2004).
[16] K. J. Tielrooij *et al.*, Phys. Rev. Lett. **102**, 198303 (2009).
[17] R. Car and M. Parrinello, Phys. Rev. Lett. **55**, 2471 (1985).
[18] Y. Liu, D. A. Yarne, and M. E. Tuckerman, Phys. Rev. B **68**, 125110 (2003).
[19] H. S. Lee and M. E. Tuckerman, J. Phys. Chem. A **110**, 5549 (2006).
[20] H. S. Lee and M. E. Tuckerman, J. Chem. Phys. **125**, 154507 (2006).
[21] H. S. Lee and M. E. Tuckerman, J. Chem. Phys. **126**, 164501 (2007).
[22] J. G. Grossman *et al.*, J. Chem. Phys. **120**, 300 (2004).
[23] Y. A. Mantz, B. Chen, and G. J. Martyna, J. Phys. Chem. B **110**, 3540 (2006).
[24] S. Woutersen and H. J. Bakker, Phys. Rev. Lett. **96**, 138305 (2006).
[25] A. D. Becke, Phys. Rev. A **38**, 3098 (1988).
[26] C. Lee, W. Yang, and R. G. Parr, Phys. Rev. B **37**, 785 (1988).
[27] N. Troullier and J. L. Martins, Phys. Rev. B **43**, 1993 (1991).
[28] M. Tuckerman, A. Chandra, and D. Marx, Acc. Chem. Res. **39**, 151 (2006).
[29] G. J. Martyna, M. E. Tuckerman, and M. L. Klein, J. Chem. Phys. **97**, 2635 (1992).
[30] M. E. Tuckerman *et al.*, Comput. Phys. Commun. **128**, 333 (2000).
[31] B. Halle and G. Karlström, J. Chem. Soc., Faraday Trans. II **79**, 1031 (1983).
[32] S. Izvekov and G. A. Voth, J. Chem. Phys. **123**, 044505 (2005).
[33] S. Meiboom, J. Chem. Phys. **34**, 375 (1961).
[34] T. Steinel *et al.*, J. Phys. Chem. A **108**, 10 957 (2004).
[35] S. Woutersen and H. J. Bakker, Phys. Rev. Lett. **83**, 2077 (1999).
[36] C. J. Fecko *et al.*, Science **301**, 1698 (2003).
[37] D. Laage and J. T. Hynes, Science **311**, 832 (2006).
[38] D. Laage and J. T. Hynes, J. Phys. Chem. B **112**, 14 230 (2008).